

Published in final edited form as:

Nano Lett. 2008 December ; 8(12): 4593–4596.

Targeted Gold Nanoparticles enable Molecular CT Imaging of Cancer

Rachela Popovtzer^{*,1}, Ashish Agrawal², Nicholas A. Kotov², Aron Popovtzer³, James Balter³, Thomas. E. Carey⁴, and Raoul Kopelman^{*,1}

¹Department of Chemistry, University of Michigan, Ann Arbor, MI, USA

²Department of Chemical Engineering, University of Michigan, Ann Arbor, MI, USA

³Department of Radiation Oncology, University of Michigan, Ann Arbor, MI, USA

⁴Department of Otolaryngology/ Head and Neck Surgery, University of Michigan, Ann Arbor, MI, USA

Abstract

X-ray based computed tomography (CT), is among the most convenient imaging/diagnostic tools in hospitals today in terms of availability, efficiency and cost. However, in contrast to magnetic resonance imaging (MRI) and various nuclear medicine imaging modalities, CT is not considered a molecular imaging modality since targeted and molecularly specific contrast agents have not yet been developed. Here we describe a targeted molecular imaging platform that enables, for the first time, cancer detection at the cellular and molecular level with standard clinical CT. The method is based on gold nano-probes that selectively and sensitively target tumor selective antigens, while inducing distinct contrast in CT imaging (increased x-ray attenuation). We present an *in vitro* proof of principle demonstration for head and neck cancer, showing that the attenuation coefficient for the molecularly targeted cells is over 5 times higher than for identical but untargeted cancer cells or for normal cells. We expect this novel imaging tool to lead to significant improvements in cancer therapy, due to earlier detection, accurate staging and micro-tumor identification.

Imaging plays a critical role in overall cancer management; in diagnostics, staging, radiation planning and evaluation of treatment efficiency. Standard clinical imaging modalities such as CT, MRI and ultrasound, can be categorized as structural imaging modalities; they are able to identify anatomical patterns and to provide basic information regarding tumor location, size and spread based on endogenous contrast. However, these imaging modalities are not efficient in detecting tumors and metastases that are smaller than 0.5 cm, and they can barely distinguish between benign and cancerous tumors¹.

Molecular imaging is an emerging field that integrates molecular biology with *in vivo* imaging, in order to gain information regarding biological processes and to identify diseases based on molecular markers, which usually appear before the clinical presentation of the disease. Currently, positron emission tomography and single photon emission tomography are the main molecular imaging modalities in clinical use, however, they provide only functional information regarding molecular processes and metabolites, which is indirect and nonspecific to distinct cells or diseases^{2, 3}. Recently, various types of targeted nano-probes have been developed for optical and MRI molecular imaging, such as superparamagnetic nanoparticles⁴⁻⁷; quantum dots⁸⁻¹⁰ and gold nanoparticles as cancer optical imaging probes¹¹⁻¹³.

*Corresponding Author: Raoul Kopelman; kopelman@umich.edu Phone: 734-764-7541. Fax: 734-936-2778.

CT is one of the most useful diagnostic tools in hospitals today in terms of availability, efficiency and cost. Currently, CT is not a molecular imaging modality, since relevant targeted and molecularly specific contrast agents have not yet been developed. Present CT contrast agents are predominantly based on iodine containing molecules, which are effective in absorbing X-rays; however, they are nonspecifically targeted since they cannot be conjugated to most biological components or cancer markers and they allow only very short imaging times due to rapid clearance by the kidneys.

Gold induces a strong X-ray attenuation, as was first demonstrated, inadvertently, by Wilhelm Roentgen, in the first x-ray human image (Figure 1). Gold nanoparticles have in addition, unique physical, chemical and biological properties, which make them an ideal candidate for CT contrast agents. The ability of CT to distinguish between different tissues is based on the fact that different tissues provide different degrees of X-ray attenuation, where the attenuation coefficient is determined by the atomic number and electron density of the tissue; the higher the atomic number and electron density, the higher the attenuation coefficient. The atomic number and electron density of gold (79 and 19.32 g/cm³, respectively) are much higher than those of the currently used iodine (53 and 4.9 g/cm³). Note that for CT imaging the total amount of gold per unit volume (voxel) is the only important parameter, regardless of the shape of the particles. In addition, gold nanoparticles provide a high degree of flexibility in terms of functional groups for coating and targeting, and have also proved to be nontoxic and biocompatible *in vivo* ^{14, 15}.

Recent progress towards nanotechnology based CT imaging has been made by Hainfeld *et al* ¹⁶; they demonstrated the feasibility of gold nanoparticles to induce *in vivo* vascular contrast enhancement in CT imaging, however the gold particles were not targeted as they were not conjugated to specific biomarkers. More recently, hybrid nanoparticles such as antibiofouling polymer-coated gold nanoparticles ^{17, 18}, gadolinium coated gold nanoparticles ¹⁹, PEG coated nanoparticles ²⁰ and polymer-coated Bi₂S₃ nanoparticles ²¹ have been developed as vascular CT contrast agents.

In this study we describe a new platform for *in vivo* CT molecular imaging, based on new class of immuno-targeted gold nanoprobes that selectively and sensitively target tumor specific antigens. These gold nanoprobes form a concentrated assembly on the cancer cells, yielding a distinguishable X-ray attenuation, which is not typical for non-decorated cells or tissue. This transforms the targeted cancer into highly distinct and easy to diagnose features.

While a CT molecular imaging agent would potentially have broad applicability for many cancer types, for this research we have chosen to work with head and neck cancer, which is the fifth most common cancer worldwide ²². Squamous cell carcinoma (SCC) represents more than 90% of all head and neck cancers. Many SCC of the head and neck present as advanced tumors for which the true extent is difficult to determine from present CT and physical examination. Cure rates for oral cancers have declined ²³ in recent years and better diagnostic tools are needed for accurate staging and discovery of tumor extent. Previously it has been demonstrated that SCC is characterized by significant over-expression of the A9 antigen ²⁴, which is also called the alpha6beta4 integrin ²⁵, and that there is a strong correlation between the A9 expression level and metastatic behavior ²⁶. It has also been demonstrated that the UM-A9 antibody can home onto SCC tumors *in vivo* ²⁷. An additional reason for choosing head and neck cancer was because one of its major diagnostic challenges today is a reliable detection of involved lymph nodes, since their status is one of the most important prognosis predictors, and is also critical for appropriate treatment. However, assessment of lymph nodes based on structural imaging features is limited in sensitivity and specificity and fails to distinguish between non-neoplastic and malignant processes. These limitations lead to the routine performance of prophylactic procedures such as extensive neck dissection and radiation, and,

on the other hand, a lack of treatment for undiagnosed small metastases which is the first cause of the reappearance of cancer. Hence, the development of more sensitive *in vivo* imaging techniques is of major importance, and could substantially improve head and neck cancer diagnosis, treatment and potential cure.

In these experiments, we synthesized gold nanorods (AuNR) and conjugated them with UM-A9 antibodies, which home specifically to SCC head and neck cancer²⁷. We examined their feasibility to effectively induce contrast enhancement in CT imaging, as a specific and sensitive targeted probe in head and neck cancer. Note that for CT imaging the total amount of gold per unit volume (voxel) is the only important parameter, regardless the shape of the particles. AuNR are more advantageous in comparison with spherical nanoparticles because they offer a complementary method of detection for some cancers based on their IR adsorption^{28, 29}. Most importantly, in comparison with other techniques utilizing optical properties of AuNR, CT scans are not limited by the depth of cancer in the tissue.

Gold nanorods fabrication

AuNR were synthesized using the seed mediated growth method³⁰. The mean length was 45 nm and the mean diameter was 15 nm with gold concentration of 2.5 mg/mL. Antibody conjugation: The bio-conjugation of the AuNR to the UM-A9 antibody was achieved according to the method described by Kim et al.³¹. Briefly, a layer of biocompatible³²⁻³⁴ polyacrylic acid (PAA) is adsorbed onto the surface of gold nanorods followed by addition of EDC/NHS. PAA coated nanorods were dispersed in 1ml of PBS (pH 6.0) buffer followed by 100uL (N-ethyl-N'-(3-dimethylaminopropyl)carbodiimide) EDC and 100uL of 0.2M (N-hydroxy-succinimide) NHS mixture to provide active sites on gold nanorods that undergo amidation reaction with the antibodies. The amount of antibody added is 20µg per 1.96mg of molecular gold. The mixture was stored overnight in refrigerator at 4°C followed by centrifugation and redispersion in ultrapure water to remove unbound antibody in the solution.

Cell culture

UM-SCC-1 and UM-SCC-5 human head and neck cancer cell lines and the negative control samples of fibrosarcoma (UM-FS-1) and melanoma (UM-Mel-1), which are known not to express the A9 antigen, were cultured in DMEM media supplemented with 10% fetal bovine serum, 1mM sodium pyruvate, 100 units/ml penicillin, 100 µg/ml streptomycin sulfate and 292 µg/ml L-glutamine (all from InVitrogen, Carlsbad CA).

Cells-AuNR binding

One milliliter of cell suspension (10^6 cells/mL) was mixed with 1mL of antibody-coated AuNR solution (2.5 mg/mL), and allowed to interact for 90 min at room temperature. Then, the solution was 3 times centrifuged at 1000 rpm for 5 min, to wash out unbound antibody from the AuNR-antibody complexes; after each centrifugation step the mixture was redispersed in PBS solution (1 mL total volume).

CT scans

all scans were performed using clinical CT at 80kVp (GE Lightspeed QX/I; General Electric, Waukesha WI). The suspensions, in cuvettes, were scanned using a shaped Styrofoam assembly to hold the samples in place.

CT Imaging Experiment

Two SCC human head and neck cancer cell lines (10^6 cells/mL) were used; oral cancer UM-SCC-1 and larynx cancer UM-SCC-5. Both cancerous cell lines were shown before to have a

significant over-expression of the A9 antigen²⁴. CT imaging was performed on the SCC cells, which were targeted with the UM-A9 antibody-coated gold nanorods.

The following negative control experiments were performed: (a) CT imaging of the same head and neck cancer cells (UM-SCC-1 and UM-SCC-5) in a suspension, without the addition of nanoparticles; (b) CT imaging of the same head and neck cancer cells that were targeted with gold nanorods that are coated with antibodies that *do not match* with the SCC cells (*KHRI-3*) and (c) CT imaging of non-cancerous cells (normal fibroblast cells), and of other types of cancer cells (melanoma) that were targeted with the UM-A9 antibodies-coated gold nanorods. CT imaging of a solution of bare gold nanorods (suspended in water, without any cells) provides the positive control.

The attenuation values (HU) that were obtained from the CT imaging are shown in figure 2.

As shown in figure 2, the change in the *attenuation coefficient* (with respect to water) of the SCC cancer cells that were targeted by the A9 antibody coated gold nanorods is over 5 times higher than that of the non-targeted SCC cancer cells (32 and 28 HU vs. 168 and 172 HU, respectively). This demonstrates that the gold nanorods were attached to the cancer cells with high density, yielding a distinguishable CT attenuation number that is higher than that for typical soft tissue (typical attenuation values for solid tissue are in the range of 0-50 HU), thus making the targeted cells detectable in sufficient concentration. The attenuation values observed for the negative control samples that were targeted with gold nanorods (larynx and oral cancer cells targeted with nanorods that are coated with non matching antibodies, and normal fibroblast and melanoma cells targeted with A9 antibodies) revealed relatively low non-specific binding (58, 54, 50, 62 HU, respectively), and demonstrate that head and neck tumors may show a likely enhancement of 3-4 times the local contrast of non-targeted tissue *in vivo*. Such a specificity and local enhancement is consistent with a previous study investigating the potential use of UM-A9 as a radiolabeled imaging agent for human squamous carcinoma tumors *in vivo*²⁷. The attenuation value observed for the positive control sample, the bare gold nanorods, is 158 HU; this high number was expected since the sample contained a high concentration of gold (2.5 mg/mL).

In these experiments we tested 1 milliliter samples which contained 10^6 SCC cancer cells. Assuming the size of one SCC cancer cell is approximately 10 microns, there may be sufficient differential signal from tumors as small as 1 mm^3 to provide detectable contrast, nearly at the limit of resolution for clinical CT scanning. Another important parameter that should be noted is the high differential contrasts that have been obtained in the above experiments. The signal (HU obtained from the targeted SCC) is significantly higher than the background value (defined as the HU obtained from the control experiments). The enhancement of local signal increases local CT attenuation above the normal values for soft tissue, thus providing encouraging initial indications that sufficient specificity can be obtained in *in vivo* experiments.

Light Scattering Images of targeted and non-targeted SCC Head and Neck Cancer cells

SCC head and neck cancer cells that were targeted with UM-A9 antibody coated gold nanorods and SCC that were incubated with non-matching antibodies (R-KHRI-3) coated gold nanorods, were placed on a slide for dark field microscope imaging. Figure 3 shows, for the scattering images, clearly distinguishable differences between the specifically and selectively targeted SCC cells and those that were exposed to non-matching coated gold nanorods. The SCC cancer cells (oral and larynx cancer) that were targeted with the non-matching antibody-coated gold nanorods yielded only a small amount of scattered light, resulting from the non-specific binding. Yet, these images clearly illustrate that only the correctly conjugated nanoparticles bind specifically, with high concentrations, to the surfaces of the SCC cells.

In conclusion, these proof of principle experiments demonstrated that we may be able to identify, through CT scans, the existence of SCC cancer cells; the concentrated assembly of gold nanoparticles that form exclusively on the targeted cancer cells yield a strong selective X-ray attenuation that is distinct from the attenuation obtained by identical but untargeted cancer cells or by normal cells.

We expect that the CT molecular imaging technique will revolutionize modern head and neck cancer diagnosis and staging, by allowing reliable and sensitive detection of lymph nodes and other metastasis, which are not available today. This might also prevent or minimize the now routinely performed neck dissection, which is associated with considerable morbidity. The importance of such a technique is further reinforced because of the vast availability and the extensive use of CT in clinics today, and will provide the ability to perform simultaneously macroscopic (CT) and microscopic (molecular based CT) imaging.

Acknowledgments

This work was supported by the CRC-UM grant, UM Head and Neck Cancer SPORE NCI/NIDCR P50 CA97248, the National Science Foundation BioSensor Program, NSF-DMR 0455330 (RK), and AFOSR under MURI grant FA9550-06-1-0337.

References

1. Rusinek H, et al. Pulmonary nodule detection: Low-dose versus conventional CT. *Radiology* 1998;209:243–249. [PubMed: 9769838]
2. Al-Nahhas A, et al. Gallium-68 PET: A new frontier in receptor cancer imaging. *Anticancer Research* 2007;27:4087–4094. [PubMed: 18225576]
3. Nanni C, et al. Role of 18F-FDG-PET and PET/CT imaging in thyroid cancer. *Biomedicine & Pharmacotherapy* 2006;60:409–413.
4. Lamerichs R. MRI-based molecular imaging using nano-particles. *Cellular Oncology* 2008;30:100–100.
5. Sun C, et al. In vivo MRI detection of gliomas by chlorotoxin-conjugated superparamagnetic nanoprobe. *Small* 2008;4:372–379. [PubMed: 18232053]
6. Kopelman R, et al. Multifunctional nanoparticle platforms for in vivo MRI enhancement and photodynamic therapy of a rat brain cancer. *Journal of Magnetism and Magnetic Materials* 2005;293:404–410.
7. Koo YEL, et al. Brain cancer diagnosis and therapy with nanoplateforms. *Advanced Drug Delivery Reviews* 2006;58:1556–1577. [PubMed: 17107738]
8. Gao XH, Nie SM. Long-circulating QD probes for in-vivo tumor imaging. *Nanosensing: Materials and Devices* 2004;5593:292–299.
9. Diagaradjane P, et al. Imaging epidermal growth factor receptor expression in vivo: Pharmacokinetic and biodistribution characterization of a bioconjugated quantum dot nanoprobe. *Clinical Cancer Research* 2008;14:731–741. [PubMed: 18245533]
10. Guo Y, et al. Quantum dot conjugated hydroxylapatite nanoparticles for in vivo imaging. *Nanotechnology* 2008;19
11. Huang XH, El-Sayed IH, Qian W, El-Sayed MA. Cancer cells assemble and align gold nanorods conjugated to antibodies to produce highly enhanced, sharp, and polarized surface Raman spectra: A potential cancer diagnostic marker. *Nano Letters* 2007;7:1591–1597. [PubMed: 17474783]
12. Jain PK, El-Sayed IH, El-Sayed MA. Au nanoparticles target cancer. *Nano Today* 2007;2:18–29.
13. Huang XH, Jain PK, El-Sayed IH, El-Sayed MA. Gold nanoparticles: interesting optical properties and recent applications in cancer diagnostic and therapy. *Nanomedicine* 2007;2:681–693. [PubMed: 17976030]
14. Connor EE, Mwamuka J, Gole A, Murphy CJ, Wyatt MD. Gold nanoparticles are taken up by human cells but do not cause acute cytotoxicity. *Small* 2005;1:325–327. [PubMed: 17193451]

15. Hauck TS, Ghazani AA, Chan WCW. Assessing the effect of surface chemistry on gold nanorod uptake, toxicity, and gene expression in mammalian cells. *Small* 2008;4:153–159. [PubMed: 18081130]
16. Hainfeld JF, Slatkin DN, Focella TM, Smilowitz HM. Gold nanoparticles: a new X-ray contrast agent. *British Journal of Radiology* 2006;79:248–253. [PubMed: 16498039]
17. Kim D, Park S, Lee JH, Jeong YY, Jon S. Antibiofouling polymer-coated gold nanoparticles as a contrast agent for in vivo x-ray computed tomography imaging. *Journal of the American Chemical Society* 2007;129:7661–7665. [PubMed: 17530850]
18. Kattumuri V, et al. Gum arabic as a phytochemical construct for the stabilization of gold nanoparticles: In vivo pharmacokinetics and X-ray-contrast-imaging studies. *Small* 2007;3:333–341. [PubMed: 17262759]
19. Alric C, et al. Gadolinium chelate coated gold nanoparticles as contrast agents for both X-ray computed tomography and magnetic resonance imaging. *Journal of the American Chemical Society* 2008;130:5908–5915. [PubMed: 18407638]
20. Cai QY, et al. Colloidal gold nanoparticles as a blood-pool contrast agent for x-ray computed tomography in mice. *Investigative Radiology* 2007;42:797–806. [PubMed: 18007151]
21. Rabin O, Perez JM, Grimm J, Wojtkiewicz G, Weissleder R. An X-ray computed tomography imaging agent based on long-circulating bismuth sulphide nanoparticles. *Nature Materials* 2006;5:118–122.
22. Chin D, et al. Head and neck cancer: past, present and future. *Expert Rev Anticancer Ther* 2006;6:1111–1118. [PubMed: 16831082]
23. Carvalho AL, Nishimoto IN, Califano JA, Kowalski LP. Trends in incidence and prognosis for head and neck cancer in the United States: a site-specific analysis of the SEER database. *Int J Cancer* 2005;114:806–816. [PubMed: 15609302]
24. Kimmel KA, Carey TE. Altered Expression in Squamous Carcinoma-Cells of an Orientation Restricted Epithelial Antigen Detected by Monoclonal-Antibody A9. *Cancer Research* 1986;46:3614–3623. [PubMed: 3708592]
25. Van Waes C, et al. The A9 antigen associated with aggressive human squamous carcinoma is structurally and functionally similar to the newly defined integrin alpha 6 beta 4. *Cancer Res* 1991;51:2395–2402. [PubMed: 1750876]
26. Wolf GT, et al. Altered Antigen Expression Predicts Outcome in Squamous-Cell Carcinoma of the Head and Neck. *Journal of the National Cancer Institute* 1990;82:1566–1572. [PubMed: 2119437]
27. Wahl RL, Kimmel KA, Beierwaltes WH, Carey TE. Radioimmunodiagnosis of Human-Derived Squamous-Cell Carcinoma. *Hybridoma* 1987;6:111–119. [PubMed: 3570303]
28. Huang XH, El-Sayed IH, Qian W, El-Sayed MA. Cancer cell imaging and photothermal therapy in the near-infrared region by using gold nanorods. *Journal of the American Chemical Society* 2006;128:2115–2120. [PubMed: 16464114]
29. Gobin AM, et al. Near-infrared resonant nanoshells for combined optical imaging and photothermal cancer therapy. *Nano Letters* 2007;7:1929–1934. [PubMed: 17550297]
30. Nikoobakht B, El-Sayed MA. Preparation and growth mechanism of gold nanorods (NRs) using seed-mediated growth method. *Chemistry of Materials* 2003;15:1957–1962.
31. Kim K, Huang S-W, Ashkenazi S, O'Donnell M, Agarwal A, Kotov NA, Denny MF, Kaplan M. Photoacoustic imaging of early inflammatory response using gold nanorods. *APPLIED PHYSICS LETTERS* 2007;90
32. Chamberland DL, et al. Photoacoustic tomography of joints aided by an Etanercept-conjugated gold nanoparticle contrast agent - an ex vivo preliminary rat study. *Nanotechnology* 2008;19
33. Yoshida M, Roh KH, Lahann J. Short-term biocompatibility of biphasic nanocolloids with potential use as anisotropic imaging probes. *Biomaterials* 2007;28:2446–2456. [PubMed: 17335897]
34. Agarwal A, et al. Targeted gold nanorod contrast agent for prostate cancer detection by photoacoustic imaging. *Journal of Applied Physics* 2007;102



Figure 1. the first ever medical X-ray image (1895) taken by Roentgen
'Hand with Ring' print of Wilhelm Röntgen's first "medical" X-ray, taken on 22 December 1895. It dramatically showed the bones of her fingers; however the real size of her finger's soft tissue could be garnered from the clearly visible gold ring on her finger. Likewise, below we show that "ringing" the tumor cells with gold nanoparticles makes it effectively more visible to CT. Note that the size of the ring maps the width of the finger's soft tissue. Radiology Centennial, Inc copyrighted in 1993.

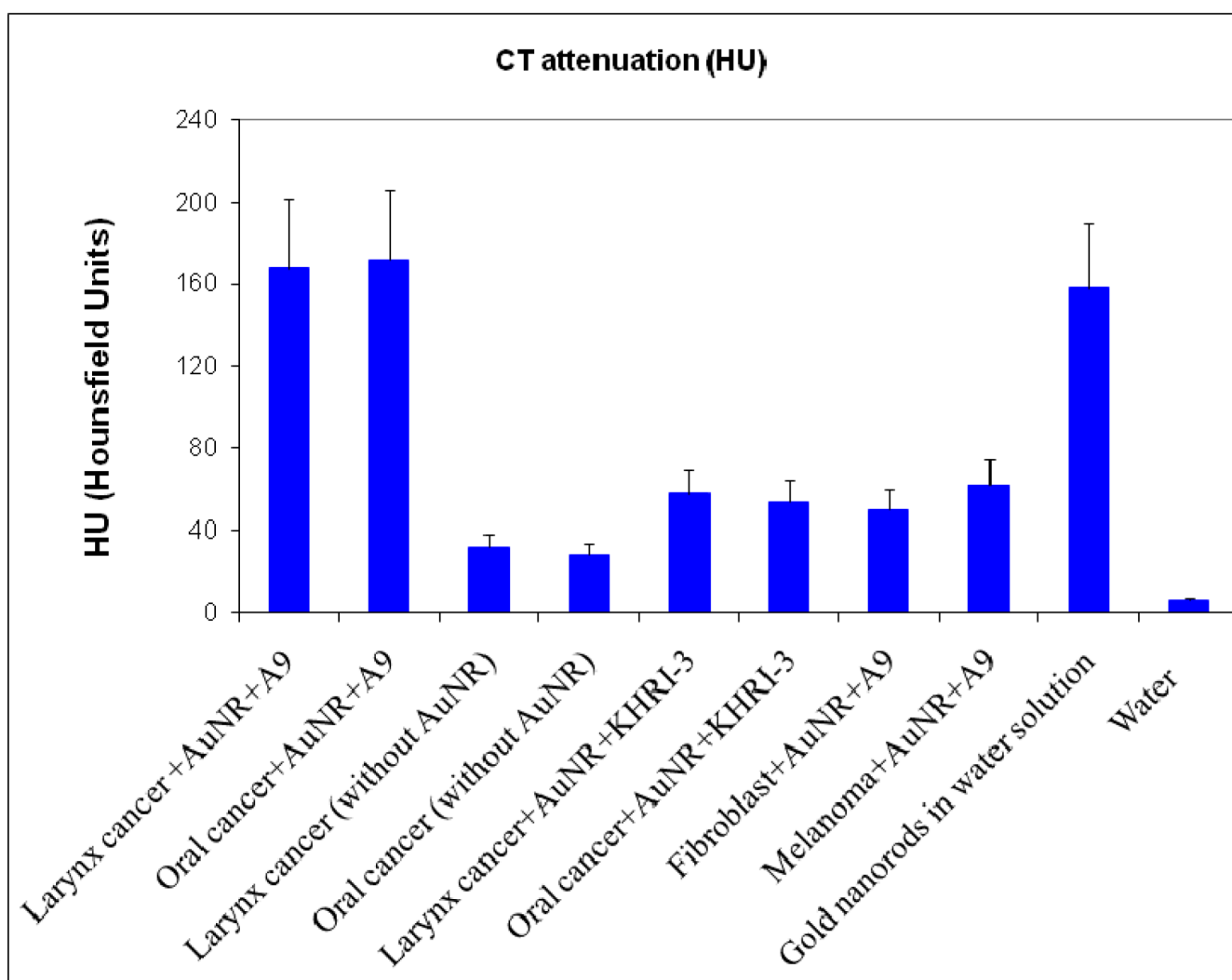


Figure 2. CT attenuation (HU) of SCC head and neck cancer cells and positive and negative control samples

Bar graph with standard deviation of 3 samples; larynx and oral cancer cells that were targeted with A9 antibody coated gold nanorods (AuNR); larynx and oral cancer cells without gold nanorods; larynx and oral cancer cells targeted with nanorods that are coated with non-matching antibodies (KHRI-3); normal fibroblast and melanoma cells targeted with A9 antibodies, bare gold nanorods in water solution (2.5 mg/mL), and water.

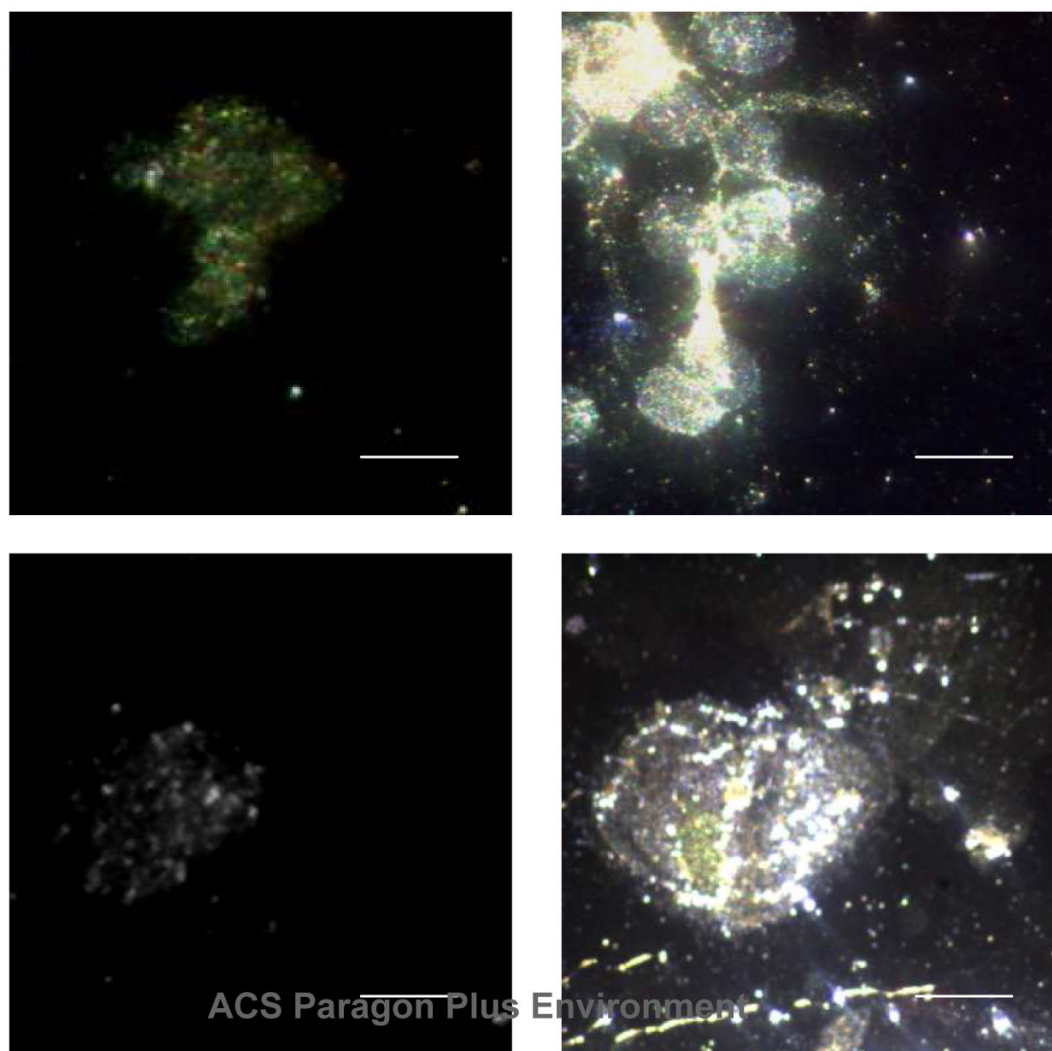


Figure 3. Dark field microscope images of SCC head and neck cancer cells

Dark field microscope images of SCC head and neck cancer cells (oral cancer upper images, larynx cancer lower images) after incubation with non-matching antibody-coated gold nanorods (left) vs. matching UM-A9 antibody-coated gold nanorods (right). Scale bar: 10 μ m